COMMISSIONING OF A DUAL-SWEEP STREAK CAMERA WITH APPLICATIONS TO THE ASTA PHOTOINJECTOR DRIVE LASER*

A. H. Lumpkin#, D. Edstrom, J. Ruan, and J. Santucci
Fermi National Accelerator Laboratory, Batavia, IL 60510, USA

Abstract

Following re-commissioning of the dual-sweep streak camera with a Gig-E readout CCD camera, a comprehensive set of measurements has been performed on the ASTA drive laser beam components with respect to bunch length, phase stability, and multiplicity of peaks. The multi-pass amplifier was identified as the primary source of the longer UV component bunch length at 4 ps and peak multiplicity. This amplifier was replaced with three single-pass amplification stages and tests indicate clean micropulses and bunch lengths of about 3.6 ps sigma.

INTRODUCTION

The high-power electron beams for the Advanced Superconducting Test Accelerator (ASTA) facility [1] will be generated in a photoinjector based on a UV drive laser and the L-band rf photocathode (PC) gun cavity. Initially, the laser was composed of a Calmar Yb fiber oscillator and amplifier, a multi-pass YLF-based amplifier (MPA), three single-pass YLF-based amplification stages, and two frequency-doubling stages that result in a UV component at 263 nm with a 3 MHz micropulse repetition rate [2]. The initial objectives of these studies were: 1) to evaluate the amplified UV component's bunch length and phase stability and 2) to commission the laser room Hamamatsu C5680 streak camera system. A Prosilica GC1380 digital CCD with Gig-E readout was used for streak camera readout as it was compatible with our image processing tools. In the following sections, the process of characterizing the UV beam using the streak camera is described. This includes identification of a UV micropulse length longer than expected, multiplicity within the bunch structure, steps taken to mitigate these issues, and UV beam characterizations following these steps. We have systematically investigated the issues of whether the multiplicity was with each micropulse of the 3 MHz train (using the gated MCP), if any multiplicity is on different cycles of the 81.25 MHz rf (using dual-sweep streak images), and the origin in the laser system of the longer bunch length and the multiplicity. We describe our extensive investigations that indicated both issues originated in the multi-pass amplifier.

EXPERIMENTAL ASPECTS

A request to have the streak camera readout camera be compatible with the Gig-E vision protocol has been addressed by selection of the Prosilica 1.3 Mpixel camera with 2/3" format. We have then used both the online Java-based ImageTool and the offline MATLAB-based ImageTool processing programs [3,4] in the commissioning of the system. Initial measurements of the UV component indicated the bunch length Gaussian fit sigma was closer to 4 ps, and there was evidence of more-than-expected peak multiplicity near the 3 MHz main peaks with spacing of 65-70 ps. Initially timing effects between the controls group 3 MHz source and that derived from the master oscillator were detected, but these were ultimately ruled out as the source of the peak multiplicity through a process of selection of individual pulses by gating the streak camera MCP and employing the dual-sweep synchroscan functions of the streak camera. Unless noted otherwise, the streak camera's synchroscan unit was phase locked to the master oscillator, which operationally provides the rf sync for the linac and rf gun. We provide a description of the commissioning of the streak camera system and image acquisition tools and the application to the drive laser.

The Drive Laser

The drive laser (Fig. 1) was based on an Yb fiber laser oscillator running at 1.3 GHz that was then divided down to 81.25 MHz and amplified. The four-stage origination and amplification was a set of commercial components from Calmar collectively referred to as the seed laser in the context of ASTA. The 81.25 MHz packets of infrared (IR) laser, at a wavelength of 1054 nm was initially directed into a YLF-based multi-pass amplifier (MPA), at 3MHz, selected by a Pockels cell referred to as the pulse picker. A number of pulses was selected using two pulse cleaner Pockels cells, while three YLF-based single-pass amplifiers (SPA) and a Northrup-Grumman SPA (NGA) boost the intensity as high as 50 µJ per pulse before the two doubling crystal stages generate the green and then the UV components at 3 MHz [2]. The UV component was transported from the laser lab through the UV transport line to the photocathode of the gun for generation of the photoelectron beams for use in the SC rf accelerator [2].

The multi-pass amplifier is a cavity that allows the amplification of the IR macropulse dependent on the timing of a fourth Pockel's cell (Conoptics 350-105) referred to as the Q-Switch. In combination with a Brewster plate, the IR beam is injected into the MPA cavity and is amplified using an YLF solid state amplifier, similar to those used in the single-pass amplification stages, until the Q Switch triggers, directing the amplified beam back out by means of the same Brewster plate, collinear with its injection trajectory. The round trip time for laser within the cavity is 12 ns, and several roundtrips-

*Work supported under Contract No. DE-AC02-07CH11359 with the United States Department of Energy.
#lumpkin@fnal.gov

ISBN 978-3-95450-133-5

generally between 8 and 14 for the purposes of these studies- are made, each resulting in a net amplification. The number of roundtrips made is adjusted by means of a T560 timing-module trigger to the Q-Switch timing. The MPA has been replaced by three single pass amplifiers.

Prosilica 1.3-Mpix Gig-E vision digital CCD which is thus compatible with the video acquisition [3,4] designed for all of the RadiaBeam beamline imaging stations. The commissioning of this readout camera as well as the image analysis tools was a primary goal of these studies.

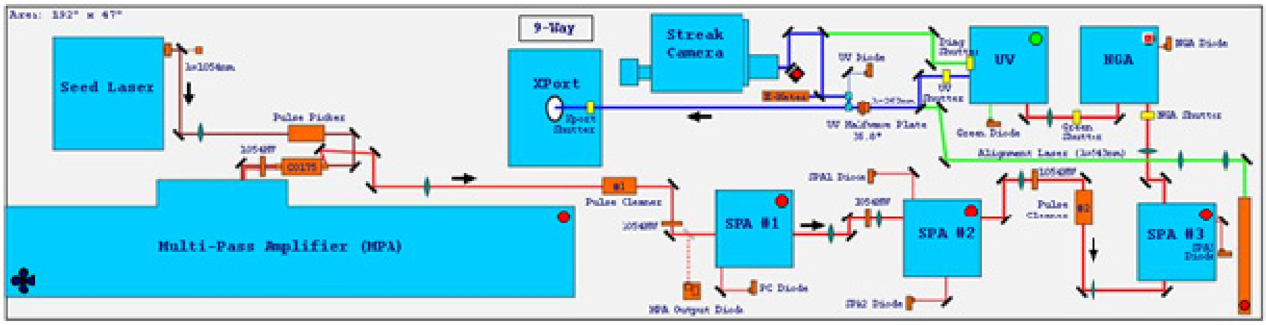

Figure 1: Schematic of the ASTA drive laser optical layout showing the seed laser, MPA, SPAs, and the streak camera.

The Hamamatsu C5680 Streak Camera System

Commissioning of the streak camera system was facilitated through a new suite of controls centered around ACNET, the Fermilab accelerator controls network. This suite included operational drivers to control and monitor the streak camera as well as Synoptic displays to facilitate interface with the driver and Java-based ImageTool programs to retrieve images from the readout camera. This commissioning period allowed for a number of improvements to be made to all aspects of interfacing with the streak camera, both in terms of front-end and back-end software, and hardware.

The streak camera consists of a Hamamatsu C5680 mainframe with S20 PC streak tube and can accommodate a vertical sweep plugin unit and either a horizontal sweep unit or blanking unit. The UV-visible input optics allow the assessment of the 263-nm component as well as the amplified green component or IR components converted to green by a doubling crystal. We started the studies with the M5675 synchroscan unit with its resonant circuit tuned to 81.25 MHz and the blanking unit. The low level rf is amplified in the camera to provide a sine wave deflection voltage for the vertical plates that results in low jitter (~1ps) of the streak camera images and allows synchronous summing of a pulse train. The temporal resolution is about 1.5 ps FWHM, or 0.6 ps sigma, for NIR photons at 800 nm. When combined with the C6878 phase locked loop (PLL) delay box we can track phase effects at the ps level over several minutes (and even hours as long as the unit phase balance is stable) and within the macropulse to about 200 fs. As a point of comparison, the M5676 vertical fast sweep unit has about 20-ps internal trigger jitter in addition to the nominal 100-ps trigger jitter of the DG535 delay units. This would mean the streak image would jitter in and out of the frame when running on the fastest sweep range with a full scale range of about 150 ps, illustrating the critical advantage of the synchroscan mode. We have replaced the Hamamatsu Peltier-cooled firewire CCD readout camera with a

There is a fundamental reduced sensitivity issue of the Prosilica camera compared to the cooled CCD camera that may push us towards the streak tube space-charge limited regime. The concept of the streak tube's using the 81.25 MHz rf from the master oscillator to generate the vertical deflection voltages with the phase-locked delay box was critical. This combination enabled a new series of experiments at A0PI [5] and will also apply at ASTA. A second set of deflection plates provides the orthogonal deflection for the slower time axis in the 100-ns to 10-ms regime. These plates are driven by the dual-axis sweep unit which was also commissioned during these studies.

In order to assess the sources of the peak multiplicity, we anticipated the use of both the streak tube's MCP gate option for the single micropulse selection and the dual-sweep mode for isolating the 81.25 MHz cycles of the synchroscan sampling mode. To examine the latter, the blanking unit was replaced with an M5679 Dual Timebase Extender unit. This unit provided a ramped horizontal deflection similar to the fast vertical deflection unit, but works over a considerably longer time-frame. The full-amplitude range for the dual-sweep unit is 0.1 µs to 100 ms. The diagram of the final streak camera configuration in Fig. 2 is representative of all studies noted hereafter, except for the gating study, where gating around one or more micropulses was selected using a DG535. In this exception, the C5680 Gate Trigger In was connected to a DG535 TTL output with the correct gating time.

Streak camera calibrations were performed with the new Prosilica readout camera through use of a Colby delay unit (PN109122; SN#8081195) to provide discrete and known ps-regime delay changes. Initially, noticeable jitter was seen on the image position with the PLL on in R1, but we took 10-, 20-, and 30-ps steps and averaged the mean positions of the images. The resulting calibration factors with 1x1 pixel binning in the CCD were: R4: 2.0 ± 0.1ps/pixel, R3: 1.0 ± 0.1 ps/pixel, R2: 0.45±0.03 ps /pixel, R1: 0.15±0.03 ps/pixel. After reducing the jitter in the system, we adjusted the R1 calibration factor's measured value.

ISBN 978-3-95450-133-5

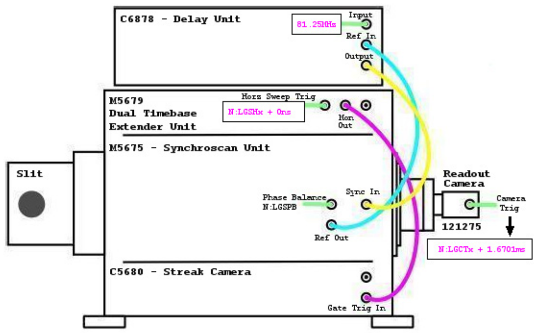

Figure 2: A streak camera wiring diagram. N:LGSHx and N:LGCTx are ACNET names for beam-synchronized VME-based timers. The 81.25MHz is derived from the Master Oscillator (MO) and an additional cable delay of 120 ns was added to N:LGSHx for the purposes of the dual sweep studies.

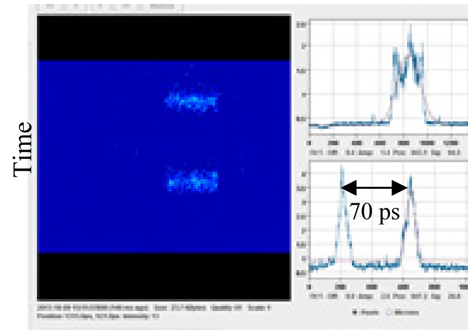

Figure 3: Example of UV multiplicity in the streak image on the left and the vertical (time) profile at lower right.

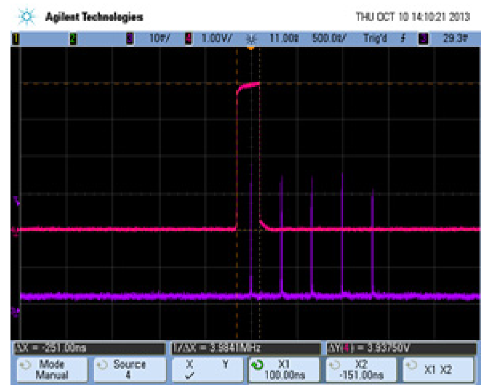

Figure 4: Screen captures of scope trace and MCP gate (250 ns) and the 5 laser micropulses detected by the photodiode. The gate width was stepped in 333-ns steps to include 1 to 5 micropulses.

EXPERIMENTAL RESULTS

Initial Amplified UV

Our laser studies began with the evaluation of the amplified UV component of the drive laser at the point before it is transmitted to the UV transport line to the rf PC gun. This is the bunch length that will determine the initial photoelectron bunch length in the gun cavity. We were aware of the possibility for space-charge effects in the streak tube with the lower Q.E of the tube PC and the lower sensitivity of the readout camera that would combine to require more input signal for the same output signal. We were able to attenuate the UV signal input to obtain focus mode slit images with a 20-μm tall slit at the 6-pixel level sigma. This value is higher than the white light (4.2 pixel) or green component value and was attributed to the inherently larger photoelectron energy spread within the tube from UV photon conversion and possibly some input optics focus. As shown in Fig. 3, the main peak was accompanied by a second peak 70 ps away in time. The assessment of whether the multiplicity was with each micropulse or just in the synchronous sum was pursued.

It was recognized that one could use the external gate mode on the streak camera which would localize the recorded image to one 300-ns interval and confirm if the multiple pulses observed are *associated with the single selected UV pulse*. Alternatively, the dual-sweep mode can be used to ascertain if any of the 5 pulses arrive on other rf cycles than one sweep. (The single sweep unit has internal trigger jitter plus DG535 trigger jitter, but in principle could be timed for one UV pulse interval). As a followup, we recorded a set of gated MCP images while running in synchroscan mode. As shown in Fig. 4, we set the gate width to 250 ns, and then the gate delay was set to include only the first of five micropulses. We observed the doublet image with only the first micropulse gated and the 7.5 ns timing shift. The gate width was progressively increased, and we generated a plot of the Gaussian fits to the amplitudes of the two peaks with doublet timing on the laser as a function of the streak camera MCP gate width for micropulses 1-5 as shown in Fig. 5. The first peak is also seen with normal timing of the laser. This monotonic increase of intensity with micropulse number as the MCP gate width was incremented in 333-ns steps confirms the assignment of the second peak to each micropulse interval.

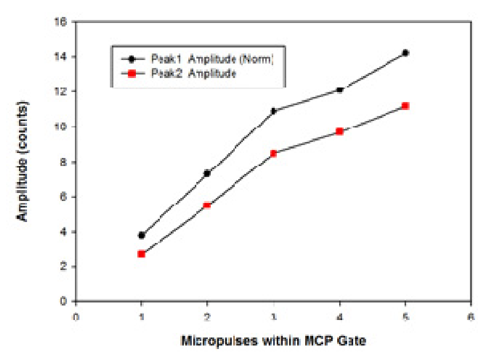

Figure 5: Plot of the two peak intensities with MCP gate width showing the doublet peak 2 tracks with each micropulse.

ISBN 978-3-95450-133-5

Amplified Green Component

An additional optical transport path was added at the location of the amplified green component to bring it to the entrance of the streak camera. Investigations of the parameters of the green component were done. With OD5.5 the focus image size was reduced to a reasonable 5.9 ± 0.2 pixels, but this is still larger than the white light value. We then proceeded to streak mode and immediately saw the multiplicity of peaks, 6-9, in the green with about 63 ± 2 ps separation on range 2. In this case the offline MATLAB program does fit the baseline even with the multiple peaks. The image bunch lengths on range 1, SS1 are longer at 40 and 37 pixels in the image below than our UV component data at ~28 pixels sigma. This is plausible with the nonlinear aspect in the frequency doubling crystal process.

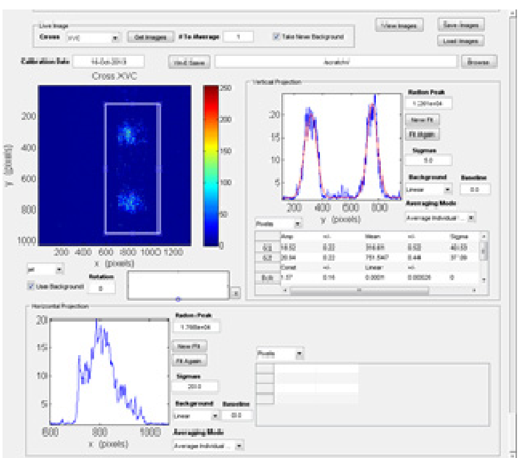

Figure 6: Amplified green component with streak camera range R1. The offline MATLAB program fit each of the peaks to Gaussians and provided amplitude, centroid, and sigma values.

Green Converted MPA Component

After confirming the seed laser output seemed nominal with 2.3-ps bunch lengths, we moved to the MPA output. As a final step, we investigated the output of the MPA after converting the IR to 527-nm light with a BBO doubling crystal. The repetition rate is 3 MHz and the signal is stronger after the MPA than the converted seed laser signal. The principal peak is about 29 pixels sigma as shown in Fig. 7 with offline analysis, so we again are in the 4.2-ps sigma bunch length regime. We adjusted the trigger timing and actually used a cable length added into the delay line to shift the trigger by 120 ns and allow clear display of the R3-100 ns image with external gate applied. The unique image is shown in Fig. 7 (upper-left quadrant). There, we still see the isolated multiplets, but the horizontal-sweep profile below the image shows three steps in the 10-image sum. Some of the peaks arrive 12.4 or 2 x12.4 ns later to the right of the first sweep cycle. There are at least 3 rf cycles represented with peaks 2 and 5 from the bottom being the brightest and usually on the *same* rf cycle and ~200 ps apart. This said, the pulse cleaners should suppress 3-MHz pulses on the adjacent rf cycles. The sum image in 8-bit scale actually has some saturation in the two brightest peaks so the relative amplitudes and the sigmas of those are overestimated.

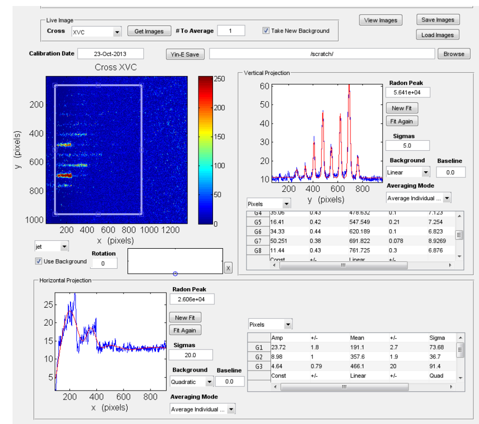

Figure 7: Dual-sweep image (R3-100ns) of the MPA output converted to green showing different intensity multiplets for different rf cycles.

UV Component with Preamp Installed

Having reviewed the data from the MPA source, we replaced the MPA with three single pass amplifiers to act as a preamp. The UV was evaluated again, and in a 200 micropulse R1 synchronous sum, we observe a bunch length of about 25.3 pixels or 3.6 ps (sigma) after subtracting in quadrature the estimated resolution term for the focus mode as shown in Fig. 8. The micropulse sum also appears clean of secondary peaks. There is a slight x-t tilt which contributes to the total bunch length.

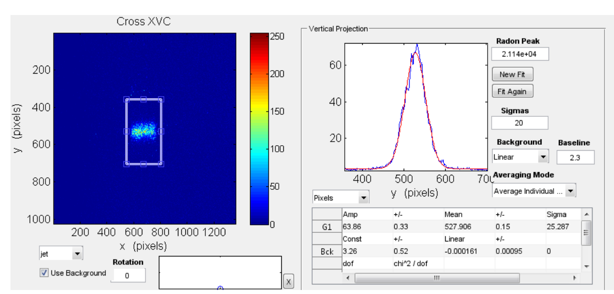

Figure 8: Synchronous UV streak image using R1 showing the reduced bunch length of 3.6 ps (sigma).

SUMMARY

In summary, we have described a series of commissioning results using the laser lab Hamamatsu streak camera with the new Prosilica Gig-E readout camera including: image processing, streak range calibrations, system phase jitter, rf phase locking, and streak-camera-based measurements of the ASTA drive laser with the multipass amplifier. We assessed the amplified UV and green, and the converted IR components from the seed laser at 81.25 MHz and the MPA output at 3 MHz. We observed a bunch-length

ISBN 978-3-95450-133-5

sigma of 4.2 ps from the MPA vs. 2.3 ps from the seed laser, and the multiplicity at 65-70 ps originating in the MPA. Implementing the preamplifier in the chain to replace the MPA mitigated these effects, and the UV laser stands ready to support the first electron beam to the 50-MeV beam dump.

ACKNOWLEDGMENTS

The authors acknowledge the acquisition of the Prosilica CCD camera for this application by Amber Johnson; the generation of ACNET streak camera, CCD, and delay box controls by C. Briegel; the development of the Java-based ImageTool code by J. Diamond, the revisions of the Matlab-based code by R. Thurman-Keup; the 81.25 MHz rf source provided by B. Chase, and the support of Elvin Harms and Nathan Eddy, all at Fermilab.

REFERENCES

[1] The ASTA User Facility Proposal, Fermilab-TM-2568, October 2013.

[2] J. Ruan, M. Church, D. Edstrom, T. Johnson, J. Santucci, "Commission of the Drive Laser System for Advanced Superconducting Test Accelerator", In *Proc. 4th Int. Particle Accelerator Conf.*, Shanghai, China, 2013, pp. 3061-3063

[3] J. Diamond, FNAL, online Java-based ImageTool, (2013).

[4] R Thurman-Keup, FNAL,offline MATLAB based. ImageTool, (2011).

[5] A.H. Lumpkin, J. Ruan, and R. Thurman-Keup, Nucl. Instr. and Meth. **A687**, 92-100 (2012).

ISBN 978-3-95450-133-5